IEEE Access
Multidisciplinary | Rapid Review | Open Access Journal

Received June 26, 2020, accepted July 18, 2020, date of publication July 30, 2020, date of current version August 13, 2020.

Digital Object Identifier 10.1109/ACCESS.2020.3013023

IEEE 802.11ba Wake-Up Radio: Performance Evaluation and Practical Designs

DER-JIUNN DENG[1], (Senior Member, IEEE), SHAO-YU LIEN[2], (Member, IEEE), CHUN-CHENG LIN[3], (Senior Member, IEEE), MING GAN[4], (Member, IEEE), AND HSING-CHUNG CHEN[5,6], (Senior Member, IEEE)

[1]Department of Computer Science and Information Engineering, National Changhua University of Education, Changhua 500914, Taiwan
[2]Department of Computer Science and Information Engineering, National Chung Cheng University, Chiayi 62102, Taiwan
[3]Department of Industrial Engineering and Management, National Chiao Tung University, Hsinchu 30010, Taiwan
[4]Huawei Technologies Company Ltd., Shenzhen 518129, China
[5]Department of Computer Science and Information Engineering, Asia University, Taichung 41354, Taiwan
[6]Department of Medical Research, China Medical University Hospital, China Medical University, Taichung 40402, Taiwan

Corresponding author: Hsing-Chung Chen (cdma2000@asia.edu.tw)

This work was supported in part by the Ministry of Science and Technology (MOST), Taiwan, under Grant MOST 107-2221-E-468-015, in part by the Asia University, Taiwan, in part by the China Medical University Hospital, China Medical University, Taiwan, under Grant ASIA-108-CMUH-05 and Grant ASIA-107-CMUH-05, and in part by the Asia University, Taiwan, Universitas Muhammadiyah Yogyakarta (UMY), Indonesia, under Grant 107-ASIA-UMY-02.

ABSTRACT Featuring a long operation time to avoid frequent battery replacements, highly energy-efficient radios have shown their pivotal functions for low-power and battery-driven devices in supporting manifold Internet-of-Things (IoT) services. To this end, prolific systems for highly energy-efficient radios have been widely deployed, but they impose a critical challenge of sacrificed data rates to preclude the applications that both require high energy efficiency and high data rates. Recently, this challenge has driven the concept of equipping two radio-chains on a low-power device, known as the *primary connectivity radio* (PCR) and *companion connectivity radio* (CCR). The PCR supports high data rate transmissions, and switches to the sleeping mode when no data should be received. In this case, the CCR stays awake to monitor traffic, and wakes up the PCR when data requiring to be received arrives. However, to practice such a concept, sophisticated operations in the physical (PHY) layer and medium access control (MAC) layers are required. Consequently, the IEEE 802.11 Task Group "ba" (TGba) has been formed to launch the normative works since 2017. In the normative development, the most challenging issue lies in the design of a new frame structure especially the preamble sequence, by which the CCR in a station (STA) can efficiently synchronize with an access point (AP) and the PCR can be promptly waken up when an AP wishes to transmit data to an STA. To comprehend such a crucial foundation for the next generation low-power IoT devices, this paper provides comprehensive knowledge of state-of-the-art PHY/MAC operations of IEEE 802.11ba. Most importantly, a preamble sequence design for synchronization is further proposed for the new frames supported in IEEE 802.11ba. Through comprehensively evaluating the performance of different designs (in terms of data rate configuration and synchronization sequences), we justify the outstanding performance of the proposed design in terms of the synchronization error rate and packet error rate, to satisfy the urgent demands in the normative works of IEEE 802.11ba.

INDEX TERMS IEEE 802.11ba, wake-up radio (WUR), wake-up frames, PHY/MAC operations, the Internet of Things, energy efficiency.

I. INTRODUCTION

The next generation Internet of Things (IoT) paradigm is projected to embrace a variety of applications, including sensors/controllers in smart cities/buildings [1], [2], intelligent transportation systems (ITS) [3]–[5], unmanned factories [6], smart agriculture, and/or smart grids [7], etc. Since these applications may involve a large number of battery-driven devices to be deployed to unreachable places by human beings, it is intractable to frequently or comprehensively replace batteries for these devices. How to efficiently prolong the lifetime of batteries therefore turns out to be an inevitable issue in practicing these IoT applications.

To tackle this issue, a considerable number of highly energy-efficient and/or low power wireless systems have been deployed, such as IEEE 802.15.4, which offers a

The associate editor coordinating the review of this manuscript and approving it for publication was Ilsun You.

transmission data rate of 250 kbps with a transmission range around 10 m. To further extend the transmission range, the low power wide area networks (LPWAN) [8] offer affordable connectivity for battery-driven devices deployed over a very wide range of geographical areas. To achieve long-range transmissions, transmission power of these battery-driven devices may need to be increased. However, to extend the lifetime of batteries, substantially increasing transmission power may be practically infeasible, and therefore LPWAN is solely suitable for IoT applications that only require to transmit a small amount of data. For example, long range (LoRa) LPWAN [9], [10] are non-standardized LPWAN systems to offer low data rates from 0.3 kbps to 50 kbps. Sigfox operates another type of LPWAN on the Industrial, Scientific, Medical (ISM) bands [11] to support an even lower data rate to transmit a small payload size of 12 bytes within up to 2 seconds. In 2014, Narrow-band IoT (NB-IoT) [12], [13] has been standardized as a part of 3GPP Release 13 to support low cost devices through reusing LTE infrastructures. The data rates of NB-IoT have been significantly enhanced as compared with that of LoRa and Sigfox, which however are only around 200 kbps. The inherent tradeoff between transmission power and data rates therefore may preclude IoT applications both requiring high energy efficiency and high data rates.

To avoid such inherent tradeoff, the two-radio-chain framework has recently received considerable attentions in the designs of low-power IoT devices [14]–[17], in which a device is equipped with two radios known as the *primary connectivity radio* (PCR) and *companion connectivity radio* (CCR). The PCR is able to support high data rates, and therefore may consume more power in long-range transmissions. To significantly enhance the energy efficiency of a low-power device, the PCR is normally in the sleeping mode, and wakes up only if there are packets to be received/transmitted by the PCR. When the PCR is in the sleeping mode, the CCR is awake to continuously monitor whether there are packets to be received by the PCR. If there are packets to be received, the CCR wakes up the PCR to perform high data rate reception. Although the concept of the two-radio-chain framework is straightforward, practicing such a system may not be an effortless task.

Since 2017, the IEEE 802.11 Task Group "ba" (TGba) has been formed to develop draft 0.1 (D0.1) of IEEE 802.11ba, which embraces MAC and PHY operations to sustain any possible upper-layer protocols and applications such as IPv6 [18], [19]. Subsequently, D1.0 has further been released since 2018 [20]. The objective of IEEE 802.11ba is to enable an active station (STA) with power consumption less than one milli-watt (mW). For this purpose, an IEEE 802.11ba STA is equipped with two radio chains known as the PCR and wake-up radio (WUR) (which is similar to the CCR). The PCR supports complete functions of legacy IEEE 802.11, and should stay in the sleeping mode for a duration as long as possible. To wake up the PCR, a new frame known as the *wake-up frame* is introduced. When an access point (AP) has packets to be transmitted to the PCR of an STA, an AP sends a wake-up frame to the WUR of an STA, then the WUR wakes up the PCR to receive packets from an AP. Although few articles have preliminarily introduced the PHY/MAC operations of IEEE 802.11ba [21]–[23], efficient designs for a wake-up frame are still open and challenging issues. To comprehend such a crucial technology for the next generation low-power IoT wireless systems, the contribution of this paper includes the followings.

- Firstly, essential knowledge of the PHY (including physical layer convergence procedure (PLCP) Protocol Data Unit (PPDU) of wake-up frames, waveform, modulation, synchronization sequence design, and data rate configuration) and MAC (including wake-up procedure, WUR beacon, WUR mode, WUR re-discovery, and channel access) procedures of IEEE 802.11ba is provided.
- Secondly, through conducting complete link-level simulations, this paper evaluates the performance for different synchronization sequence designs and data rate configurations of the wake-up frame, to show the adequacy of these designs.
- Most importantly, the optimum designs of the synchronization sequences for the WUR frame are proposed.

The proposed designs therefore serve to meet the urgent needs in the normative works of IEEE 802.11ba.

The rest of this paper is organized as follows. In Sections II and III, foundations of MAC and PHY operations are offered. In Section IV, designs of synchronization sequences for WUR frames are proposed. Then, the performance evaluation of different data rate configurations for WUR frames are given in Section V. Simulation results for the proposed designs are provided in Section VI, and this paper is concluded in Section VII.

II. MAC OPERATIONS OF IEEE 802.11ba WURs

The standardization of IEEE 802.11ba involves sophisticated PHY and MAC operations. To fully comprehend this system, it is of crucial importance to understand MAC layer operations. In this section, knowledge of essential MAC layer operations is therefore provided.

A. WAKE-UP OPERATIONS

The basic wake-up procedure starts from an AP sending a wake-up frame to an STA, which occurs when an AP has packets to be transmitted to an STA. As aforementioned, the PCR of an STA is normally in the sleeping mode, and thus the WUR should stay awake to monitor a wake-up frame. When the WUR receives a wake-up frame, it does not have the capability to send a response frame back to an AP. In this case, the WUR wakes up the PCR, then the PCR sends a response frame to an AP to indicate that it is ready to receive downlink packets, as illustrated in Fig. 1.

To further reduce the power consumption in an STA, not only the PCR but also the WUR is able to switch to the sleeping mode. Nevertheless, if the WUR switches to the

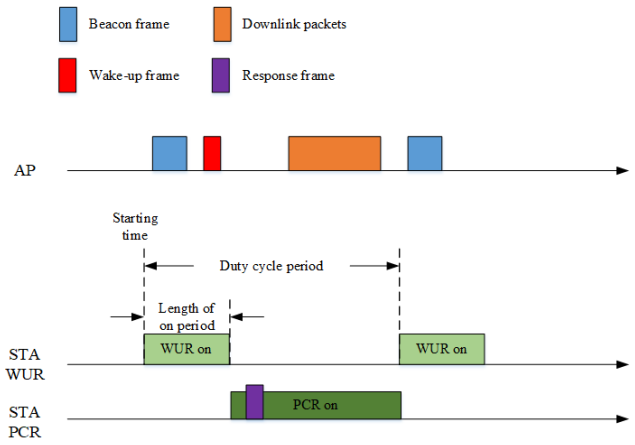

FIGURE 1. The wake-up operation in IEEE 802.11ba.

sleeping mode, then an AP may not be able to wake up an STA when there are downlink packets. To avoid such an undesirable case, an AP and an STA can exploit a negotiation procedure to decide when a WUR should wake up to check whether there are wake-up frames. This operation is know as the duty-cycle of the WUR. Since the WUR lacks the capability to transmit, the negotiation procedure is performed between an AP and the PCR. During the negotiation, four parameters for the duty cycle of the WUR are decided: 1) the **duty cycle period**, 2) the **starting time of the "on" period** (within which the WUR of an STA turns on), 3) the **length of the "on" duration**, and 4) the **minimum wake-up time** (which indicates the minimum length of the "on" period), as illustrated in Fig. 1.

To negotiate the above four parameters, an AP first advertises the **minimum wake-up duration**. Upon receiving this parameter, the PCR sends the desired values of the **length of the "on" period** and **duty cycle period** to an AP based on the constraints of energy efficiency and data reception latency. Subsequently, an AP replies the **starting time of the "on" period**. When this negotiation procedure has been completed, the STA enters to the *WUR mode* and the PCR is able to switch to the sleeping mode.

B. WUR BEACON

Once the PCR switches to the sleeping mode and only the WUR stays awake, some basic functions of the PCR also switch off, and one example is the synchronization function. STAs in a single infrastructure basic service set (BSS) are synchronized to a common clock using a mechanism called the *timing synchronization function* (TSF), which keeps the timings of all STAs in the same BSS aligned with the TSF values conveyed by a beacon frame. For this purpose, a beacon frame broadcasted by an AP is composed of a 64-bit timestamp field to represent the value of the TSF timer. Through receiving a beacon frame, each STA therefore can maintain a TSF time with modulus 2^{64} counting in increments of microseconds. Another mechanism is known as the *heart beat function*, by which an AP periodically transmits beacon frames for STAs to determine whether they are still within the coverage range of the BSS. This function also facilitates possible BSS scanning and handover procedures thereafter. Since the above two functions are not available when the STA enters the WUR mode, additional designs are needed to practice IEEE 802.11ba.

To operate the above two functions when an STA enters the WUR mode, beacon frames are necessary. For this purpose, a new beacon known as the WUR beacon frame is introduced to IEEE 802.11ba. An AP should periodically transmit the WUR beacon frame such that the WUR of an STA is able to receive the system information provided from an AP (as illustrated in Fig. 1), just like a periodic "heart beat" sequence to keep alive. If the heart beat sequence is missing at the STA side, then an STA is likely outside the coverage range of an AP, and consequently an STA needs to initiate the re-discovery procedure to find another AP. On the other hand, to achieve synchronization using the WUR, a general scheme is to include a timestamp in the WUR beacon frame. However, since the transmission rate of a beacon may be very limited, the transmission time of a 64-bit timestamp filed may occupy up to 1.024 ms, which may be a considerable burden in spectrum efficiency. To further reduce the transmission time for the timestamp filed, the WUR beacon may only carry a partial TSF for synchronization.

C. RE-DISCOVERY

As aforementioned, the hear beat function with the facilitation of WUR beacon frames enables an STA to determine whether it is still within the coverage range of the associated AP. If an STA moves outside the coverage range of an AP, then an STA needs to initiate the re-discovery procedure. The conventional re-discovery procedure in IEEE 802.11 includes scanning, authentication, and association to a BSS. In the scanning phase, the STA has to scan all the available channels to find one or more APs. However, such an operation may consume a lot of power of the STA, especially when the STA moves frequently.

To further save power during the scanning phase, a special frame known as the WUR discovery frame is introduced in IEEE 802.11ba to assist an STA to discover the BSS, and a channel is designated for this special purpose. All the APs transmit the WUR discovery frames on that special channel, which carry critical information for scanning, such as the AP's address and the AP's operating channel. Through obtaining such critical information using the WUR to monitor this special channel, an STA is able to find the AP's operating channel, then the PCR of an STA can send the authentication and association request frames. As a result, an STA is able to save power significantly.

D. WUR FRAME FORMATS

So far, this paper has introduced the WUR wake-up frame, WUR beacon frame, and WUR discovery frame. In IEEE 802.11ba, all these frames are known as *WUR frames*, and

adopt a general MAC protocol data unit (MPDU) format, as illustrated in Fig. 2.

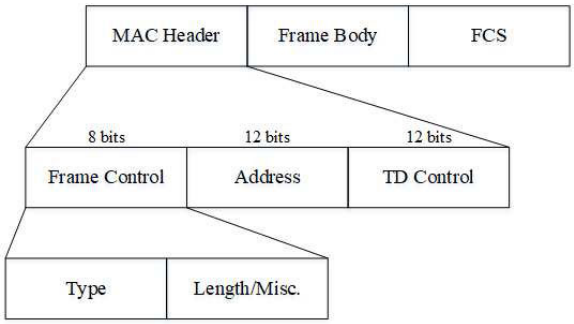

FIGURE 2. The MPDU format of a WUR frame.

Similar to the conventional IEEE 802.11 MPDU format, the MPDU of a WUR frame is composed of a MAC header, a frame body (payload), and a frame check sequence (FCS). The frame body is optional depending on the type of the WUR frame. The FCS carries the cyclic redundancy check (CRC) code of the frame, which additionally conveys the BSS identifier (BSSID) of the BSS.

The MAC header is composed of a 8-bit **frame control** field, a 12-bit **address** field, and a 12-bit **type dependent** (TD) field. The **frame control** field is further comprised of a **type** subfield and a **length/miscellaneous (Misc.)** subfield. The **type** subfield distinguishes different types of this WUR frame (e.g., WUR discovery frame, WUR wake-up frame, WUR beacon frame, etc.). The WUR discovery frame is a variable-length WUR frame, and therefore the **length/Misc.** subfield indicates the length of the **frame body**. On the other hand, the WUR wake-up frame and WUR beacon frame are constant-length WUR frames, in which the **frame body** is not present.

For the **address** field, the content depends on the type of the WUR frame. For the type of unicast WUR wake-up frame, the **address** field conveys a WUR ID (WID), which is assigned by an AP to an STA. For the type of multicast WUR wake-up frame, the **address** field conveys a group ID (GID), which is provided by an AP to identify one or more STAs. For the type of the broadcast WUR wake-up frame and the WUR beacon frame, the **address** field conveys a transmitter ID (TXID) since such a frame is provided for all the STAs. Note that the unicast WUR wake-up frame, the multicast WUR wake-up frame, and the broadcast WUT wake-up frame all belong to the type of the WUR wake-up frame, and therefore indication is required in the **length/Misc.** subfield to distinguish the broadcast WUR wake-up frames and non-broadcast WUR wake-up frames.

E. CHANNEL ACCESS

In IEEE 802.11ba, the enhanced distribute channel access (EDCA) in IEEE 802.11e is also adopted for transmitting the WUR wake-up frames. In the conventional EDCA, there are four access categories (ACs) for voice (AC-VO), video (AC-VI), best effort (AC-BE), and background (AC-BK) traffic. These ACs are also adopted by IEEE 802.11ba, by which an AP may use any AC to send the multicast WUR wake-up frames and WUR beacons. An AP may also use any AC to send a unicast WUR wake-up frame to an STA if an AP does not have any pending packets to be sent to an STA.

III. PHY OPERATIONS OF IEEE 802.11ba WUR

As aforementioned, the operations of IEEE 802.11 WUR highly rely on WUR frames. The PHY of IEEE 802.11ba therefore emphasizes on the design of WUR frames. This section introduces the waveform, preamble, and each field in the convergence procedure (PLCP) protocol data unit (PPDU) format of a WUR frame.

A. WAVEFORM OF WUR FRAMES

An AP of IEEE 802.11ba reuses the existing orthogonal frequency division multiplex (OFDM) transmitter architecture adopted by IEEE 802.11a/g/n/ac/ax to generate the OFDM waveform with 312.5 kHz subcarrier spacing. Since narrowband waveform reception can significantly reduce the power consumption at the receiver side, the narrowband OFDM waveform is generated by populating the contiguous 13 out of 64 subcarriers with null center subcarrier to occupy a 4 MHz band. In addition to power saving, this scheme also facilitates alleviation of the peak to average power ratio (PAPR) issue in OFDM. To further reduce power consumption at the receiver (STA) side, in Layer 1, the WUR frame does not carry any data information, and an AP only utilizes the OFDM waveform as transmission medium to transmit WUR frames.

For the WUR, information bits are modulated into on-off keying (OOK) symbols, and the transmitter (i.e., AP) of WUR frames uses these OOK symbols to mask the generated narrowband OFDM waveform, which is known as the multi-carrier OOK (MC-OOK) waveform. At the receiver (i.e., WUR in an STA) side, OOK demodulation does not require any channel equalization in the frequency and time domains, and therefore a non-coherent detection (such as envelope detection) is sufficient to demodulate OOK. Using the non-coherent detection, the receiver does not need to maintain/track a highly accurate oscillating rate. As a result, a phase-lock loop (PLL) could be avoided to further reduce the power consumption at the receiver side.

B. PREAMBLE OF WUR FRAMES

Different from mobile networks, such as 3GPP New Radio (NR) [24] and Long-Term Evolution (LTE), in which a user equipment (UE) should ubiquitously track the timing reference of a base station (BS) no matter whether there are uplink/downlink data transmissions or not, in an IEEE 802.11 system, an STA only maintains a coarse timing alignment with an AP by continuously receiving beacons sent by an AP. When an STA powers on, it should search and associate to an AP, and then continuously monitors the beacon

frames sent by the AP. Since a beacon frame contains the identity (ID) of the BSS (i.e., BSSID), an STA is able to distinguish the beacon frames sent by different APs through identifying the BSSID. In practical operations, an AP may not send beacons periodically. When the occasion of sending a beacon arrives but the channel has been occupied by other transmitters, the transmission of a beacon should be postponed. Following the spirits of data communications, an IEEE 802.11 system can tolerate a larger level of clock drifting between a transmitter and a receiver. Nevertheless, to ensure that an PPDU can be successfully detected, a preamble inserting into an PPDU is inevitable.

To coexist with legacy IEEE 802.11 devices in the same bands, a 20 MHz non-high throughput (non-HT) preamble is prepended in any WUR PHY PPDU. The PPDU format for WURs is illustrated in Fig. 3, which includes a **legacy short-training field** (LSTF), a **legacy long-training field** (LLTF), and a **legacy signal** (LSIG). Note that LSTF, LLTF and LSIG are not only modulated in 13 subcarriers. Instead, a WUR PPDU relies on **LSIG** to silence the legacy IEEE 802.11 devices in the same 20 MHz band up to 5.6 ms to avoid collisions, and therefore these three field are modulated to occupy 20 MHz bandwidth. However, this 20 MHz non-HT preamble cannot be recognized and decoded by a WUR due to the narrowband reception capacity. Nevertheless, the 20 MHz non-HT preamble can be used for setting the coarse automatic gain controller (AGC). On the contrary, the **synchronization** (SYNC) and **data** field are modulated using OOK waveform over 13 subcarriers, and these two field will be introduced later.

Because of the power spectral density (PSD) regulations in some regions, narrowband MC-OOK has to be transmitted at lower power. This operation leads to a sharp power drop between the 20 MHz non-HT of the preamble and the MC-OOK portion in the WUR PPDU. Such a power drop is called signal/carrier loss, which may degrade the performance of protection from being interfered by other legacy IEEE 802.11 devices. On the other hand, if the power level of the legacy preamble is lowered to the level of the MC-OOK portion, the LSIG protection region could be harmed. To bridge the power gap between 20 MHz non-HT preamble and narrowband MC-OOK portion, an additional 20 MHz OFDM symbol with 312.5 kHz subcarrier spacing and binary phase shift keying (BPSK) is added in the middle of the PPDU format.

C. DATA FIELD IN PPDU

Since a WUR frame carries only the control information, the **data** field in a WUR PPDU is used to carry the control information, instead of data. In the WUR PPDU format, both **SYNC** and **data** fields are MC-OOK waveforms. **SYNC** is used to help the WUR to synchronize with WUR frame, and to know the position of the **data** field. For **SYNC**, the lowest data rate is applied to facilitate the robustness. For **data**, multiple data rates can be applied to achieve either better spectrum efficiency or better coverage (reliability). For the sake of simplicity, two data rates for the **data** field are supported by WUR: 250 kbps and 62.5 kbps, as illustrated in Fig. 3. The higher data rate can be accommodated for short range communications to enhance the spectrum efficiency, while the lower data rate facilitates coverage extension, especially in the outdoor environment. Section IV will justify these two data rates for the **data** field.

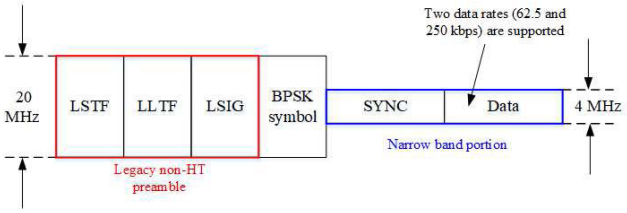

FIGURE 3. The PPDU format of a WUR frame.

To further improve the performance of envelope detection of the WUR, the Manchester code can be applied to the **data** field. There are two engineering merits of applying the Manchester code: 1) Estimation of MC-OOK detection threshold is not required for the Manchester code, and a long period of "zero" waveform can be avoided to to overcome the drawback of OOK symbol transmission over the unlicensed spectrum.

D. SYNC FIELD IN PPDU

Since only two data rates are supported in the **data** field, the preamble designs for WUR are simplified. It is possible to allow "zero" **LSIG** field such that the preamble only contains the **SYNC** field, which is used to boost the synchronization at the WUR side. A simple way to have zero **LSIG** field is that the **LSIG** field is composed of only pre-defined sequences to differentiate the two data rates. Taking complexity into the implementation consideration, a single correlator is preferred at the WUR. In the following section, we will evaluate the performance of different designs for synchronization sequences, and propose a design to effectively improve the error rate of synchronization.

IV. OPTIMUM SYNCHRONIZATION SEQUENCE DESIGNS FOR WUR FRAMES

There are two possible schemes to differentiate the two data rates in the **data** field through the **SYNC** field under the constraint of using only one correlator at the WUR. The first scheme is to have different synchronization sequences with different durations, and the duration of the **SYNC** field depends on the data rate of the **data** field. When the low data rate is used for the **data** field, the duration of the SYNC field is 128 μs (denoted as SYNC1). When the high data rate is used for the **data** field, the duration of the **SYNC** field is 64 μs (denoted as SYNC2). The purpose of using a longer **SYNC** duration (SYNC1) to denote the low data rate of **data** is to achieve a better reliability performance, while a shorter **SYNC** duration (SYNC2) associated with the high data rate of **data** achieves a better spectrum efficiency. For example,

suppose that **data** has a 48-bit payload. If SYNC2 for the high data rate reduces from 128 μs (as compared with SYNC1) to 64 μs, then the packet duration is reduced by 20%. Since the WUR frame does not carry data, the preamble may be regarded as overheads. Therefore, for a better spectrum efficiency, the overall length of a WUR PPDU should be as short as possible. Please also note that, since an STA may not know whether the data rate of the received WUR frame before successfully detecting the **SYNC** field, and there are two possible lengths of the **SYNC** field (i.e., 64 μs and 128 μs), the required time to detect an WUR frame is at least 128 μs.

The first scheme consists of two steps: 1) Design a base sequence $\mathbb{Z}$ (of 1s and 0s) of a length N, and 2) construct SYNC1 and SYNC2 based on $\mathbb{Z}$ and its complementary $1-\mathbb{Z}$. In the following proposition, a possible design for SYNC1 and SYNC2 is provided.

Proposition 1: One possible design is that SYNC1 is the concatenation of two $\mathbb{Z}$ sequences (i.e., SYNC1 $=$ $[\mathbb{Z}\ \mathbb{Z}]$), and SYNC2 $=[1-\mathbb{Z}]$. The receiver correlates the received signal with the template $(2\mathbb{Z}-1)$, and there are two possible results at the output of the correlator if the received signal is the WUR frame. When SYNC1 is received, then there are two positive peaks at the correlator output. On the other hand, when SYNC2 is received, there is only one negative peak.

Example 1: Following ***Proposition 1****, we take*

$$\mathbb{Z}=[00010110101000111010111100100110] \quad (1)$$

as a demonstration example, and the normalized correlation output with MC-OOK waveform (the bit duration is 2 μs) is shown in Fig. 4.

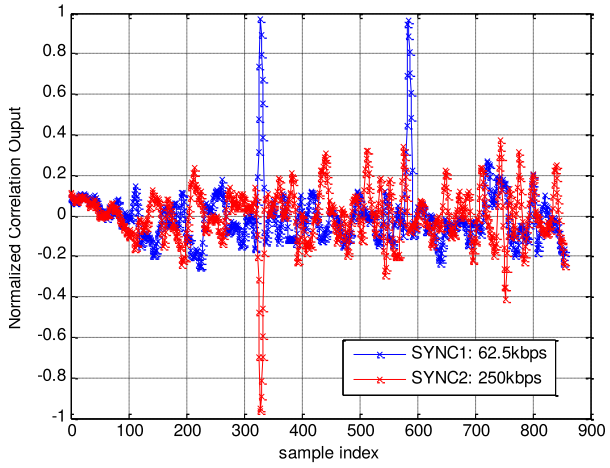

FIGURE 4. **The normalized correlation output of the first scheme in designing the synchronization sequence.**

With the facilitation of these designs, the timing can be derived by detecting the peak of the correlator output after carrier sensing within a window.

The second scheme is to designate the complementary synchronization sequences (i.e., SYNC2) having the same duration as that of SYNC1. In this scheme, packet acquisition is determined by the maximum magnitude of the correlator output, and the data rate for the payload part is determined by the sign of the correlator output which has the maximum magnitude. To ensure these complementary synchronization sequences to achieve the optimum synchronization performance, auto-correlation metrics should be adopted as the time acquisition, and date detection is directly related to the auto-correlation peak condition. Based on the characteristics of the complementary synchronization sequences, this paper proposes two metrics for choosing the best preamble sequence as follows:

$$\textbf{ACmetric}^{+} \triangleq \frac{\max[x(n)]}{\max[\mathbf{x}\setminus\max[|x(n)|]]}, \quad (2)$$

$$\textbf{ACmetric}^{-} \triangleq \frac{\min[x(n)]}{\max[\mathbf{x}\setminus\max[|x(n)|]]} \quad (3)$$

for all n and $x(n)\in\mathbf{x}$, where $x(n)$ is the value of the correlator output at time step n, and $\mathbf{x}$ is the set of all possible values of $x(n)$. Since the data rates of the **data** field can be detected by the sign of the correlator output, $\textbf{ACmetric}^{+}$ is the metric used when the correlator output is positive, while $\textbf{ACmetric}^{-}$ is used when the correlator output is negative. The numerator of Eqn. (2) is the largest value among all $x(n)$, while the numerator of Eqn. (3) is the smallest value among all $x(n)$. In both Eqn. (2) and Eqn. (3), the denominators are the second largest value of $|x(n)|$ in $\mathbf{x}$, and therefore both Eqn. (2) and Eqn. (3) can be regarded as the ratios of the largest correlator output to the second largest correlator output. With the above metrics, a few complementary sequences with the optimum $\textbf{ACmetric}^{+}$ and $\textbf{ACmetric}^{-}$ can be obtained. In the following example, one of the optimum complementary sequence is demonstrated.

Example 2: Taking

$$\text{SYNC1}=[10100011011011110000100111000101] \quad (4)$$

as an example, SYNC2 $=1-$ SYNC1 can be the optimum sequence. In this case, the receiver performs the similar procedure as that in the first scheme to correlate the received signal with template $(2\times$ SYNC1 $-1)$. There are two possible results for the correlator output if the received signal is a WUR frame. If SYNC1 is transmitted, then there is one positive peak appearing at the correlator output, as shown in Fig. 5. Alternatively, if SYNC2 is transmitted, there is one negative peak at the correlator output, as shown in Fig. 6.

In general, the second scheme performs better than the first scheme, since there could be construction loss in designing a long synchronization sequence. Section VI will study the performance of different sequence designs for the second scheme. Please note that, to identify the existence of a WUR frame, the WUR of an STA should continuously perform the correlation operation on the received signals. If the output of the correlation operation does not exceed a threshold, the received signal is regarded as interference or noise, and a WUR frame is not identified.

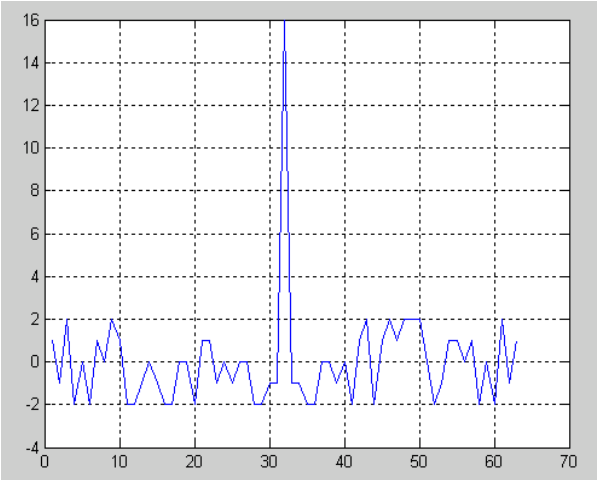

FIGURE 5. The output of the correlator when the input is SYNC1 (in which the horizontal axis denotes the sample index, and the vertical axis denotes the result of correlation output).

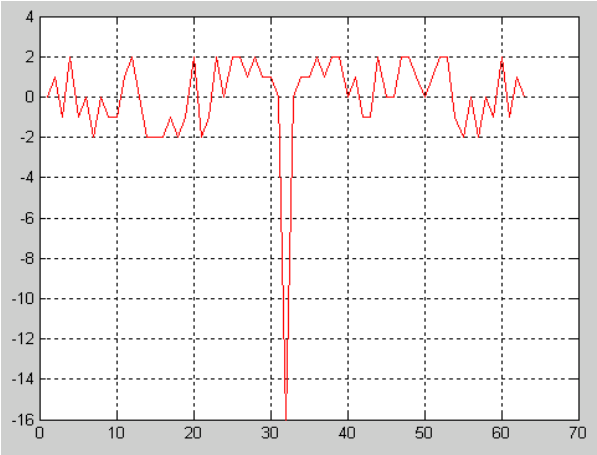

FIGURE 6. The output of the correlator when the input is SYNC2 (in which the horizontal axis denotes the sample index, and the vertical axis denotes the result of correlation output).

V. DATA RATE DESIGNS FOR Data FIELD IN WUR FRAMES

This section continues the discussion on how to designate the values of the high date rate and low date rate of the **data** field in the PPDU of a WUR frame. This investigation can be proceeded through conducting the following simulations.

We first investigate how to decide the value of the high data rate for the **data** field from the perspective of the available link margin (ALM). For this investigation, the adopted simulation parameters and assumptions are summarized in Table 1. In this investigation, two different data rates, 500 kbps and 250 kbps, are considered as candidates for the high data rates. The simulation results for different carrier frequencies (i.e., 2.4 and 5 GHz) and different distances (d) between a transmitter and a receiver are summarized in Table 2. We can observe from Table 2 that 250 kbps data rate offers better ALMs as compared with that of the 500 kbps data rate. We can also observe that the cross points of the 250 kbps data rate are 105 m and 70 m at carrier frequencies

TABLE 1. Parameters and assumptions for simulation study to decide the value of high data rate.

Parameter	Value
Carrier frequency	2.4 GHz and 5 GHz
Transmission power	15 dBm
Path loss model	IEEE 802.11ax channel model [25]
Transmission/reception antenna gain	0 dB
Bandwidth (w)	4 MHz
Noise power (N_0)	-174+10log$w$ dB
Noise floor (NR)	-108 dB
Noise figure (NF)	10 dB

TABLE 2. Available link margin under different data rates.

2.4 GHz/5 GHz	$d = 10$ m	$d = 30$ m	Cross point
ALM for 500 kbps	33 dB/27 dB	14 dB/8 dB	73 m/48 m
ALM for 250 kbps	38 dB/32 dB	19 dB/13 dB	105 m/70 m

2.4 GHz and 5 GHz, respectively, both of which are larger than those in the 500 kbps data rate. These results thus reveal that, for the high data rate, 250 kbps can be more effective as compared with higher values.

Next, we investigate how to decide the value of the low data rate for the **data** field. Since a major requirement for the WUR deployment is to coexist with legacy IEEE 802.11 networks. In other words, the transmission range of a WUR is expected to be around the same level of that of legacy IEEE 802.11. To select the adequate value of the low data rate, the regional regulations should be considered. In Table 3, regulations of unlicensed bands in different regions are summarized. Based on the power spectral density (PSD) and equivalent isotropic radiated power (EIRP), we can observe the followings.

- Over the 4 MHz bandwidth, the transmission power level is 4 dB lower than that over the 20 MHz bandwidth in the 2.4 GHz carrier frequency.
- Over the 4 MHz bandwidth, the transmission power level is 7 dB lower than that over the 20 MHz bandwidth in the 5 GHz carrier frequency.
- A lower transmission power level may result in a higher probability of idle status in PHY clear channel assessment (CCA) check in the existing 20 MHz bandwidth, as compared with that of the conventional IEEE 802.11 packet.

Hence, more protection is required for wake-up frame from being interfered by coexisting IEEE 802.11 systems. Moreover, a 8 dB loss and a 3 dB loss can be estimated due to the receiver noise figure and OOK detection, respectively. Therefore, there are 15 dB loss (31.6 x) in 2.4 GHz and 18 dB loss (63 x) in 5 GHz for WURs. Since the lowest data rate in the existing OFDM-based IEEE 802.11 is 6 Mbps over the 20 MHz, the 62.5 kbps data rate is therefore decided for WURs after a careful calculation.

VI. SIMULATION RESULTS OF SYNCHRONIZATION SEQUENCE DESIGNS

In this section, we evaluate the performance of the proposed synchronization sequence in **Proposition 1** and **Example 2** in Section IV, which is optimum with respect to Eqn. (2)

TABLE 3. Communication regulations of unlicensed spectrum in different regions.

Region	Band (GHz)	Power limit of AP (dBm)	PSD limit of AP (dBm/MHz)	20 MHz 802.11 (dBm)	4 MHz WUR (dBm)	Δ (dBm)
FCC	2.4	30	N/A	30	30	0
FCC	5.15-5.25	30	17	30	23	-7
FCC	5.25-5.35	24	11	24	17	-7
FCC	5.47-5.725	24	11	24	17	-7
FCC	5.725-5.85	30	33	30	30	0
ETSI	2.4	20	10	20	16	-4
ETSI	5.15-5.25	23	10	23	16	-7
ETSI	5.25-5.35	23	10	23	16	-7
ETSI	5.47-5.725	30	17	30	23	-7
China	2.4	20	10	20	16	-4
China	5.15-5.25	23	10	23	16	-7
China	5.25-5.35	23	10	23	16	-7
China	5.725-5.85	30	13	26	19	-7

TABLE 4. Parameters and Assumptions for performance evaluation of different synchronization sequence designs [27]–[29].

Parameter	Value
Number of channels	1
Symbol length	4 μs
Data rate of **data**	250 kbps
Modulation	OOK
Sampling rate	20 samples per OOK symbol
Channel upsampling rate	400 samples per OOK symbol
Channel model	Ch.D NLOS in IEEE 802.11ax channel model [25]
Common frequency offset	+/-200 ppm
Transmission/reception filter	5th order Butterworth
Cutoff frequency of filter	2.5 MHz
Sampling rate of filter	50 MHz
Front silence period	2 ms
False alarm rate	$< 1\%$
Power consumption of WUR in received mode	< 1mW
Number of simulation replications	1000
CFO	+/- 200 ppm

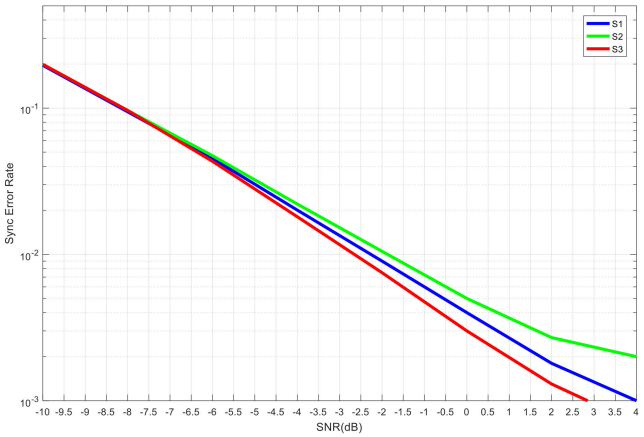

FIGURE 7. The synchronization error rate when $N = 2$.

and Eqn. (3). In this performance evaluation, the parameters and assumptions for the simulations are provided in Table 4, and the selected complementary sequences is compared with the other two pairs of complementary sequences: 31-bit M-sequences [26] with one more 0 and random sequence. The selected basic sequence SYNC 1 and the basis sequences of other two complementary sequences are listed in the following:

- **[31-bit M-sequence]:**
  S1 = [0111010100001001011001111100011 0]
- **[Random sequence]:**
  S2 = [1011000011100110101111010001 0010]
- **[Proposed sequence]:**
  S3 = [1010001101101111000010011100010 1]

A. SYNCHRONIZATION ERROR RATE

In Figs. 7 and 8, we evaluate the performance in terms of the synchronization error rate for the three synchronization sequence designs, where a synchronization error occurs when one of the following conditions is met.

1) max(|correlation output|) is less than a threshold (which is set to 2 in our simulations).
2) SYNC1 is detected as SYNC2, or SYNC2 is detected as SYNC1.
3) Timing acquisition error over the 50 MHz (filter) sampling rate is larger than a certain value N.

For $N = 2$, it can be observed from Fig. 7 that the proposed design achieves a performance gain of 1 dB and 3 dB as compared with M-sequence and random sequence. For $N = 0$ in Fig. 8, the performance gain of the proposed design is around 0.5 to 4 dB as compared with M-sequence and random sequence. These performance gains thus demonstrate the effectiveness of the proposed designs.

B. PACKET ERROR RATE

In Fig. 9, we further evaluate the performance in terms of the packet error rate (PER) for the three synchronization sequence designs, where a packet error occurs when one of the following conditions is met.

1) max(|correlation output|) is less than a threshold (which is set to 2 in our simulations).
2) SYNC1 is detected as SYNC2, or SYNC2 is detected as SYNC1.
3) The number of bit error in one packet is larger than zero.

It can also be observed from Fig. 9 that the performance gain of the proposed design is around 0.5 to 1.5 dB as compared with M-sequence and random sequence. This result also suggests the practicability of the proposed design.

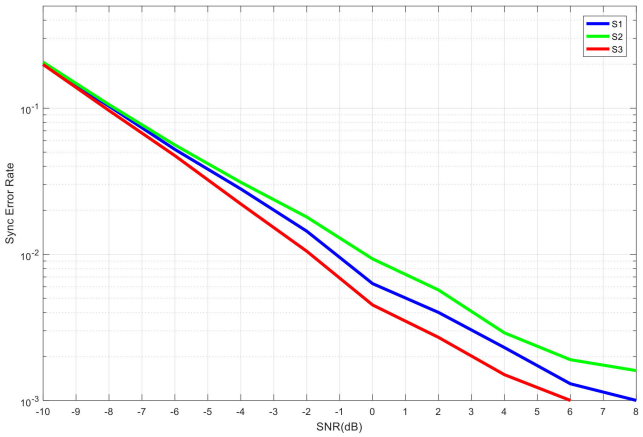

FIGURE 8. The synchronization error rate when $N = 0$.

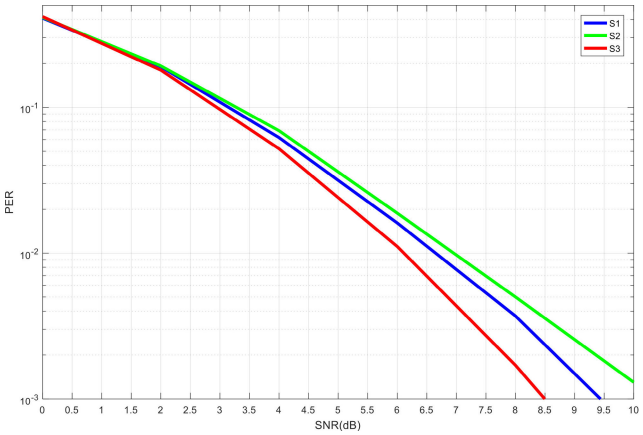

FIGURE 9. The packet error rates of different designs.

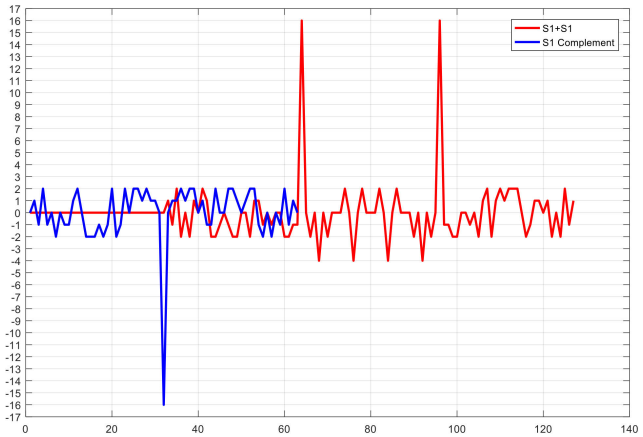

FIGURE 10. The output of the correlator when S1 is used (in which the horizontal axis denotes the sample index, and the vertical axis denotes the result of correlation output).

C. ANALYSIS OF CORRELATION OUTPUTS

In Fig. 10 to Fig. 12, the analysis results of the outputs of auto-/cross-correlation at the STA side under different sequence designs of the **SYNC** field (i.e., S1, S2 and S3) are provided. This analysis is conducted using the parameters provided

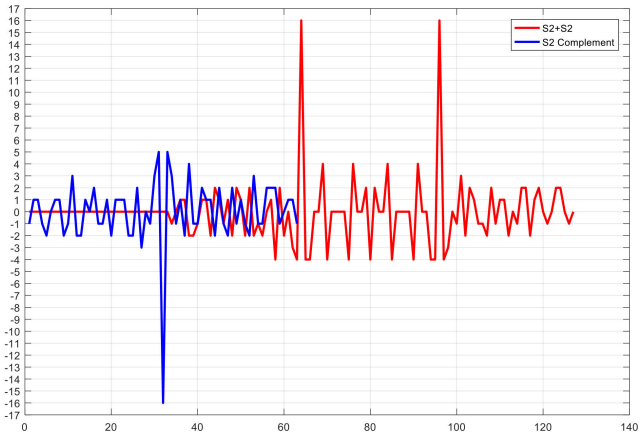

FIGURE 11. The output of the correlator when S2 is used (in which the horizontal axis denotes the sample index, and the vertical axis denotes the result of correlation output).

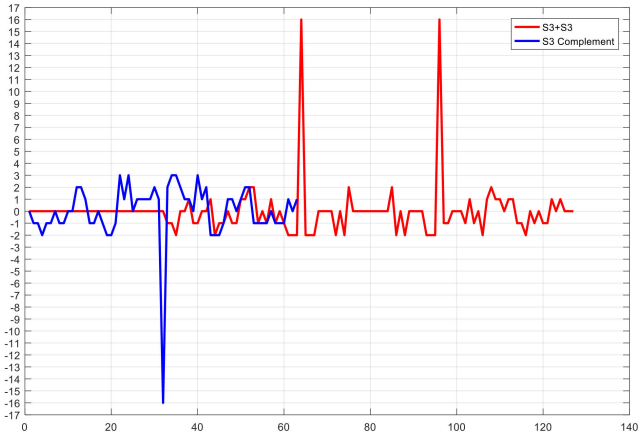

FIGURE 12. The output of the correlator when S3 (proposed design) is used (in which the horizontal axis denotes the sample index, and the vertical axis denotes the result of correlation output).

in Table 4, except that the low data rate of the **data** field (i.e., 62.5 kbps) is considered instead of the high data rate (i.e., 250 kbps), as the performance for the high data rate has been justified in Fig. 7 to Fig. 9. If we express the analysis results in Fig. 10 to Fig. 12 in terms of the metric (2) for the low data rate, then the outputs are 4, 4, and 8 for S1, S2, and S3, respectively. In other words, the proposed design S3 provides the best performance as compared with that of M-sequence and random sequence. These results are particularly insightful for the practical deployment of IEEE 802.11ba, since the low data rate is used for coverage extension and this feature is very crucial for a low power system.

VII. CONCLUSION

This paper has presented the insightful knowledge of the PHY/MAC operations of IEEE 802.11ba WUR, which includes the procedures of wake-up operations, WUR beacon transmissions, WUR mode, re-discovery and channel access in the MAC layer, and waveform, modulation, and preamble designs in the PHY layer. Moreover, this paper also proposed

the optimum practical synchronization sequence designs for the WUR frames, in which two synchronization sequences (to discriminate two different data rates in the **data** field of an PPDU) are of the same length and are complementary with each other. The simulation results fully demonstrated that the proposed designs provided better performance in terms of the synchronization error rate and PER as compared with that of the random sequence and M-sequence. In addition, through link-level simulations, this paper also justified that the present high data rate value of the **data** field in an PPDU of a WUR frame (i.e., 250 kbps) was adequate to achieve better spectrum efficiency in terms of the ALM as compared with that of higher data rates. In the meantime, the present low data rate value of the **data** field in an PPDU of a WUR frame (i.e., 62.5 kbps) was feasible to facilitate coverage extension by taking different regional communication regulations into considerations.

REFERENCES

[1] J. Kang, J. Kim, and M. Sohn, "Supervised learning-based lifetime extension of wireless sensor network nodes," *J. Internet Services Inf. Secur.*, vol. 9, no. 4, pp. 59–67, Nov. 2019.

[2] C.-S. Shih, J.-J. Chou, and K.-J. Lin, "WuKong: Secure run-time environment and data-driven IoT applications for smart cities and smart buildings," *J. Internet Services Inf. Secur.*, vol. 8, no. 2, pp. 1–17, May 2018.

[3] R. Sanchez-Iborra, J. S. Gomez, J. Santa, P. J. Fernandez, and A. F. Skarmeta, "Integrating LP-WAN communications within the vehicular ecosystem," *J. Internet Services Inf. Secur.*, vol. 7, no. 4, pp. 45–56, Nov. 2017.

[4] C.-S. Shih, W.-Y. Hsieh, and C.-L. Kao, "Traceability for vehicular network real-time messaging based on blockchain technology," *J. Wireless Mobile Netw., Ubiquitous Comput., Dependable Appl.*, vol. 10, no. 4, pp. 1–21, Dec. 2019.

[5] M. Giliberto, F. Arena, and G. Pau, "A fuzzy-based solution for optimized management of energy consumption in e-bikes," *J. Wireless Mobile Netw., Ubiquitous Comput., Dependable Appl.*, vol. 10, no. 3, pp. 45–64, Sep. 2019.

[6] B. B. Sánchez, R. Alcarria, D. S. de Rivera, and Á. S. Picot, "Enhancing process control in industry 4.0 scenarios using cyber-physical systems," *J. Wireless Mobile Netw.*, vol. 7, no. 4, pp. 41–64, 2016.

[7] M. S. Rahman, A. Basu, T. Nakamura, H. Takasaki, and S. Kiyomoto, "PPM: Privacy policy manager for home energy management system," *J. Wireless Mobility Netw., Ubiquitous Comput. Dependable Appl.*, vol. 9, no. 2, pp. 42–56, 2018.

[8] Q. M. Qadir, T. A. Rashid, N. K. Al-Salihi, B. Ismael, A. A. Kist, and Z. Zhang, "Low power wide area networks: A survey of enabling technologies, applications and interoperability needs," *IEEE Access*, vol. 6, pp. 77454–77473, 2018.

[9] L. Feltrin, C. Buratti, E. Vinciarelli, R. D. Bonis, and R. Verdone, "LoRaWAN: Evaluation of link- and system-level performance," *IEEE Internet Things J.*, vol. 5, no. 3, pp. 2249–2258, Jun. 2018.

[10] M. Pulpito, P. Fornarelli, C. Pomo, P. Boccadoro, and L. A. Grieco, "On fast prototyping LoRaWAN: A cheap and open platform for daily experiments," *IET Wireless Sensor Systems*, vol. 8, no. 5, pp. 237–245, Oct. 2018.

[11] M. Centenaro, L. Vangelista, A. Zanella, and M. Zorzi, "Long-range communications in unlicensed bands: The rising stars in the IoT and smart city scenarios," *IEEE Wireless Commun.*, vol. 23, no. 5, pp. 60–67, Oct. 2016.

[12] M. Chen, Y. Miao, Y. Hao, and K. Hwang, "Narrow band Internet of Things," *IEEE Access*, vol. 5, pp. 20557–20577, 2017.

[13] S. Popli, R. K. Jha, and S. Jain, "A survey on energy efficient narrowband Internet of Things (NBIoT): Architecture, application and challenges," *IEEE Access*, vol. 7, pp. 16739–16776, 2018.

[14] R. Piyare, A. L. Murphy, C. Kiraly, P. Tosato, and D. Brunelli, "Ultra low power wake-up radios: A hardware and networking survey," *IEEE Commun. Surveys Tuts.*, vol. 19, no. 4, pp. 2117–2157, Sep. 2017.

[15] F. Z. Djiroun and D. Djenouri, "MAC protocols with wake-up radio for wireless sensor networks: A review," *IEEE Commun. Surveys Tuts.*, vol. 19, no. 1, pp. 587–618, 1st Quart., 2017.

[16] V. Jelicic, M. Magno, D. Brunelli, V. Bilas, and L. Benini, "Benefits of wake-up radio in energy-efficient multimodal surveillance wireless sensor network," *IEEE Sensors J.*, vol. 14, no. 9, pp. 3210–3220, Sep. 2014.

[17] M. Magno, V. Jelicic, B. Srbinovski, V. Bilas, E. Popovici, and L. Benini, "Design, implementation, and performance evaluation of a flexible low-latency nanowatt wake-up radio receiver," *IEEE Trans. Ind. Informat.*, vol. 12, no. 2, pp. 633–644, Apr. 2016.

[18] Z. Yan, S. Zhang, H. Zhou, H. Zhang, and I. You, "Network mobility support in PMIPv6 network," in *Proc. 6th Int. Wireless Commun. Mobile Comput. Conf.*, Jun. 2010, pp. 890–894.

[19] I. You, Y. Hori, and K. Sakurai, "Enhancing SVO logic for mobile IPv6 security protocols," *J. Wireless Mobility Netw., Ubiquitous Comput. Dependable Appl.*, vol. 2, no. 3, pp. 26–52, 2011.

[20] *Wireless LAN medium access control (MAC) and physical layer (PHY) specifications: Wake-up radio operation*, document P802.11ba Draft 1.0, Oct. 2018.

[21] S. Hwang, I. Kim, K.-M. Kang, and S. Park, "Wake-up latency evaluation of IEEE 802.11ba WUR system," in *Proc. Int. Conf. Inf. Commun. Technol. Converg. (ICTC)*, Oct. 2018, pp. 880–882.

[22] D. K. McCormick, "Preview: IEEE technology report on wake-up radio," in *Proc. Technol. Report Wake-Up Radio*, 2017, pp. 1–4.

[23] H. Hong, Y. Y. Kim, and R. Y. Kim, "A low-power WLAN communication scheme for IoT WLAN devices using wake-up receivers," *Appl. Sci.*, vol. 8, no. 72, pp. 1–16, Jan. 2018.

[24] S.-Y. Lien, S.-L. Shieh, Y. Huang, B. Su, Y.-L. Hsu, and H.-Y. Wei, "Toward ubiquitous massive accesses in 3GPP machine-to-machine communications," *IEEE Commun. Mag.*, vol. 55, no. 6, pp. 64–71, Jun. 2017.

[25] *IEEE 802.11ax Channel Model Document*, Sep. 2014.

[26] S. W. Golomb and G. Gong, *Signal Design for Good Correlation: For Wireless Communication, Cryptography, and Radar*. Cambridge, U.K.: Cambridge Univ. Press, 2005.

[27] *Multiple Data Rates for WUR*, Standard IEEE 802.11-17/0654r0, May 2017.

[28] *WUR Preamble SYNC Field Design*, Standard IEEE 802.11-17/0983r0, Jul. 2017.

[29] *Simulation scenario and evaluation methodology*, Standard IEEE 802.11-17/0188r9, Jul. 2017.

DER-JIUNN DENG (Senior Member, IEEE) received the Ph.D. degree in electrical engineering from National Taiwan University, in 2005. He joined the Department of Computer Science and Information Engineering, National Changhua University of Education, as an Assistant Professor, in August 2005. He was a Distinguished Professor, in August 2016. In August 2018, he was with Overseas Chinese University, as the Dean of the Research and Development, for a period of one year. He was also with the Department of Industrial Technology, Ministry of Economic Affairs, as an Advisor, for a period of two years. His research interests include multimedia communication, quality-of-service, and wireless local networks. He is a Fellow of EAI. He received the number of research awards, such as the Research Excellency Award and the Outstanding Faculty Research Award from the National Changhua University of Education, the ICS 2014 Best Paper Award, the NCS 2017 Best Paper Award, and the Chinacom 2017 Best Paper Award. He serving on several program chairs, symposium chairs, and technical program committees of the IEEE, EAI, and other international conferences. He serves as the Co-Editor-in-Chief for *EAI Endorsed Transactions on IoT* and *Journal of Computers*. He also serves as an Associate Editor for the *IEEE Network Magazine* and the *International Journal of Communication Systems*.

SHAO-YU LIEN (Member, IEEE) received the B.S. degree from National Taiwan Ocean University, in 2004, the M.S. degree from National Cheng Kung University, in 2006, and the Ph.D. degree from National Taiwan University, in 2011. He joined National Taiwan University and the Massachusetts Institute of Technology (MIT), as a Postdoctoral Researcher. He has been a 3GPP Standardization Delegate in LTE, LTE-A, LTE Pro, and 5G NR, since 2009. He was with National Formosa University, as an Assistant Professor and an Associate Professor, from 2013 to 2017. He is currently with National Chung Cheng University, as an Associate Professor. He was a leading organizers of number of technical workshops, such as the IEEE VTC-Spring, in 2015, the IEEE CLOBECOM, in 2015, Qshine, in 2015 and 2016, the IEEE PIMRC, in 2017, the IEEE GLOBECOM, in 2019, and the IEEE ICC, in 2020. He has contributed more than 70 technical documents and patents in conjunction with HTC Corporation, the Institute for Information Industry (III), the Industrial Technology Research Institute (ITRI), and Huawei. His research contribution on radio access congestion control has been officially included with EU FP7 Project EXALTED and three of the IEEE journal articles listed with ESI Highly Cited Paper. His research interests include configurable networks, cyber-physical systems, radio access networks, and robotic networks. He received the number of prestigious research recognitions, including the URSI AP-RASC 2013 Young Scientist Award, the IEEE Communications Society Asia-Pacific Outstanding Paper Award, in 2014, the Scopus Young Researcher Award (Elsevier), in 2014, the IEEE ICC 2010 Best Paper Award, and the IEEE Tainan Section Best Young Professional Member Award, in 2019. He serves as a Guest Editor for *Wireless Communications and Mobile Computing (WCMC)*, in 2017, and the IEEE TRANSACTIONS ON COGNITIVE COMMUNICATIONS AND NETWORKING, in 2019.

CHUN-CHENG LIN (Senior Member, IEEE) received the B.S. degree in mathematics, the M.B.A. degree in business administration, and the Ph.D. degree in electrical engineering from National Taiwan University, in 2000, 2007, and 2009, respectively. He was with the National Kaohsiung University of Science and Technology, from 2009 to 2010. He was also an Assistant Professor of computer science with the University of Taipei, from 2010 to 2011. He joined National Chiao Tung University, in 2011. He has been a Professor of industrial engineering and management, since 2016. He has also been an Associate Dean of the College of Management, National Chiao Tung University, since 2017. His main research interests include wireless networks, information visualization, design and analysis of algorithms, and computational management science.

MING GAN (Member, IEEE) received the Ph.D. degree from the University of Science and Technology of China, Hefei, China, in 2014. From September 2012 to September 2013, he was a Visiting Ph.D. Student with Northwestern University, Evanston, IL, USA. He is currently a Senior Principle Engineer with Huawei Technologies Company Ltd. He has published more than 80 accepted proposals in the IEEE 802.11. He is dedicated to the research on 802.11be (WiFi 7), 802.11ax (WiFi 6), 802.11ba, and full duplex. His research interests include network coding, compressed sensing, optimization theory, the Internet of Things, and wifi. He is a Voting Member of the IEEE 802.11 Standard Association Working Group.

HSING-CHUNG CHEN (Senior Member, IEEE) received the Ph.D. degree in electronic engineering from National Chung Cheng University, Taiwan, in 2007. From February 2008 to July 2018, he was an Assistant Professor and an Associate Professor with the Department of Computer Science and Information Engineering, Asia University, Taiwan, where he has been a Distinguished Full Professor and the Chairman with the Department of Bioinformatics and Medical Engineering, since May 2014. He has also been a Full Professor with the Department of Computer Science and Information Engineering, Asia University, from August 2018 to July 2019, where he has been a Distinguished Full Professor and the Chairman (Director) with the Department of Computer Science and Information Engineering, since August 2019. He was a Research Consultant with the Department of Medical Research, China Medical University Hospital, China Medical University, Taichung, Taiwan. His current research interests include information and communication security, cyberspace security, blockchain network security, the Internet of Things application engineering and security, mobile and wireless networks protocols, medical and bio-information signal image processing, artificial intelligence and soft computing, and applied cryptography. Since February 2017, he has been a Permanent Council Member of the Taiwan Domain Names Association (Taiwan DNA), Taiwan. He is also a member of the Taiwan Fuzzy Systems Association (TFSA), ICCIT, and CCISA or IET. He received the Best Paper Awards from BWCCA, in 2018, MobiSec, in 2017, BWCCA, in 2016, and the Best Journal Paper Award from the Association Algorithm and Computation Theory (AACT). He served as the Program Committee Chair for APNIC44, organized by the Asia-Pacific Network Information Centre (APNIC), in September 2017.